

Molecular biogeography of the fungus-dwelling saproxylic beetle *Bolitophagus reticulatus* indicates rapid expansion from glacial refugia

JONAS EBERLE^{1,✉}, MARTIN HUSEMANN^{2,✉}, INKEN DOERFLER^{3,4}, WERNER ULRICH^{5,✉}, JÖRG MÜLLER^{6,7}, CHRISTOPHE BOUGET⁸, ANTOINE BRIN⁹, MARTIN M. GOSSNER^{10,18}, JACOB HEILMANN-CLAUSEN¹¹, GUNNAR ISACSSON¹², ANTON KRISTÍN¹³, THIBAUT LACHAT^{10,14}, LAURENT LARRIEU^{15,16}, ANDREAS RIGLING^{17,18}, JÜRGEN SCHMIDL¹⁹, SEBASTIAN SEIBOLD^{20,21}, KRIS VANDEKERKHOVE²² and JAN CHRISTIAN HABEL^{1,*}

¹Evolutionary Zoology, Department of Biosciences, University of Salzburg, Salzburg, Austria

²Center of Natural History, University of Hamburg, Hamburg, Germany

³Institute of Biology and Environmental Sciences, Carl von Ossietzky University, Oldenburg, Germany

⁴Terrestrial Ecology Research Group, Department of Ecology and Ecosystem Management, Technical University of Munich, Freising, Germany

⁵Department of Ecology and Biogeography, Nicolaus Copernicus University, Toruń, Poland

⁶Field Station Fabrikschleichach, Department of Animal Ecology and Tropical Biology, Julius-Maximilians-University Würzburg, Rauhenbrach, Germany

⁷Bavarian Forest National Park, Grafenau, Germany

⁸INRAE, 'Forest Ecosystems' Research Unit, Nogent-sur-Vernisson, France

⁹Engineering School of PURPAN, UMR 1201 Dynafor INRAE-INPT, University of Toulouse, Toulouse, France

¹⁰Forest Entomology, Swiss Federal Research Institute WSL, Birmensdorf, Switzerland

¹¹Center for Macroecology, Evolution and Climate, GLOBE Institute, University of Copenhagen, Copenhagen, Denmark

¹²Swedish Forest Agency, Hässleholm, Sweden

¹³Institute of Forest Ecology SAS, Zvolen, Slovakia

¹⁴School of Agricultural, Forest and Food Sciences HAFL, Bern University of Applied Sciences, Zollikofen, Switzerland

¹⁵University of Toulouse, INRAE, UMR DYNAFOR, Castanet-Tolosan, France

¹⁶CNPF-CRPF Occitanie, Tarbes, France

¹⁷Forest Dynamics, Swiss Federal Research Institute WSL, Birmensdorf, Switzerland

¹⁸Institute of Terrestrial Ecosystems, ETH Zurich, Universitätsstrasse 16, 8092 Zurich, Switzerland

¹⁹Ecology Group, Department Biology, University of Erlangen-Nuremberg, Erlangen, Germany

²⁰Ecosystem Dynamics and Forest Management, Technical University of Munich, Freising, Germany

²¹Berchtesgaden National Park, Berchtesgaden, Germany

²²Research Institute for Nature and Forest INBO, Geraardsbergen, Belgium

Received 24 December 2020; revised 16 February 2021; accepted for publication 16 February 2021

The geographical distributions of species associated with European temperate broadleaf forests have been significantly influenced by glacial–interglacial cycles. During glacial periods, these species persisted in Mediterranean and extra-Mediterranean refugia and later, during interglacial periods, expanded northwards. The widespread saproxylic

*Corresponding author: E-mail: JanChristian.Habel@sbg.ac.at

beetle *Bolitophagus reticulatus* depends closely on European temperate broadleaf forests. It usually develops in the tinder fungus *Fomes fomentarius*, a major decomposer of broadleaf-wood. We sampled *B. reticulatus* in sporocarps from European beech (*Fagus sylvatica*) and Oriental beech (*Fagus orientalis*) across Europe and the Caucasus region. We analysed mitochondrial gene sequences (*cox1*, *cox2*, *cob*) and 17 microsatellites to reconstruct the geographical distribution of glacial refugia and postglacial recolonization pathways. We found only marginal genetic differentiation of *B. reticulatus*, except for a significant split between populations of the Caucasus region and Europe. This indicates the existence of past refugia south of the Great Caucasus, and a contact zone with European populations in the Crimean region. Further potential refugia might have been located at the foothills of the Pyrenees and in the Balkan region. Our genetic data suggest a phalanx-wise recolonization of Europe, a reflection of the high mobility of *B. reticulatus*.

ADDITIONAL KEYWORDS: biogeography – broadleaf forest – expansion – *Fomes fomentarius* – genetic analysis – mobility – phalanx-wise – refugia.

INTRODUCTION

The glacial/interglacial cycles of the Pleistocene caused severe range shifts of most species across Europe (Hewitt, 1999, 2000; Schmitt, 2007; Schmitt & Varga, 2012). Many European species persisted through past glacial periods in Mediterranean refugia (Hewitt, 1999), as well as in extra-Mediterranean refugia in central Europe (Schmitt & Varga, 2012). In addition, the Ponto-Caspian area has been proposed as a potential glacial refugium for European taxa (Tarkhnishvili *et al.*, 2012; Neiber & Hausdorf, 2015). These range modifications resulted in inter- and intraspecific genetic signatures, such as differentiation through long-term isolation in disjunct glacial refugia (Hewitt, 2000). Range expansions after glacial periods are also reflected in the genetics of species. They follow two propagation patterns. The first is a pioneer process (with the two types, stepping-stone and leptokurtic), implying repeated founder effects in the wake of population expansions into new habitat patches (Ibrahim *et al.*, 1996). This propagation pattern creates typical signatures of gradual loss of genetic diversity in the course of colonization (Ibrahim *et al.*, 1996). In contrast, phalanx-wise colonization implies area-wide expansion, and therefore an absence of genetic signatures along colonization routes (Hewitt, 2000).

The biogeography of broadleaf tree species has been intensively studied in recent years (Pott, 2000; Brunet *et al.*, 2010). Forests dominated by broadleaf species currently occur in diverse ecoregions and include the Atlantic, central European, Balkan, Baltic, Dinaric and Caucasus mixed forests, all of which are characterized by typical plant, fungus and animal species (Brunet *et al.*, 2010; Müller *et al.*, 2013) that had persisted in disjunct glacial refugia. Tree species with high cold tolerances, such as birch (*Betula* sp.), occurred in extra-Mediterranean and northern refugia during the glacial stages (Svenning *et al.*, 2008; Giesecke *et al.*, 2017). Relatively thermophilic tree species, such as European

beech (*Fagus sylvatica*), survived the glacial stages in various disjunct Mediterranean refugia, as well as in a number of cryptic extra-Mediterranean refugia along the edge of the Eastern Alps, the Balkan Peninsula and northern Spain (Magri *et al.*, 2006, 2008; Saltr  *et al.*, 2013). After the last glacial period, European beech recolonized central and northern Europe mainly from the Balkan region (Magri *et al.*, 2006), while the populations in the western Mediterranean area, such as northern Spain, played a rather minor role as potential sources for recolonization (Magri *et al.*, 2006, 2008; Saltr  *et al.*, 2013).

While the biogeographical history of all tree species forming the European broadleaf forests has been well studied (Magri *et al.*, 2006, 2008; Svenning *et al.*, 2008; Saltr  *et al.*, 2013; Giesecke *et al.*, 2017), comparably little data and evidence on the biogeographical history of animal species relying on European broadleaf forests are available (Stauffer *et al.*, 1999; Rukke, 2000; Drag *et al.*, 2011, 2015, 2018; Pons *et al.*, 2011; Jim nez-Alfaro *et al.*, 2018). Moreover, in many of these studies the Caucasus region has not been considered, even though further refugia could have been located in this region.

In this study we analysed the genetic structure of the darkling beetle, *Bolitophagus reticulatus* (Linnaeus, 1767) (Tenebrionidae, Tenebrionini, Bolitophagini), a typical representative of the fauna of European broadleaf forests. The larvae and adults live in polypore fungi, usually the tinder fungus *Fomes fomentarius* (L.) Fr. 1849 (Nilsson, 1997; Midtgaard *et al.*, 1998). The beetle species is widespread across the Palaearctic region and is very mobile (Jonsson, 2003). We sampled individuals across its Western Palaearctic distribution range, including the Caucasus region. We analysed mitochondrial DNA (mtDNA) sequences and polymorphic microsatellites allowing the investigation over different rates of evolution. Based on these data, we identify past glacial refugia and range expansions during interglacial periods. In particular, we aimed to answer the following questions:

1. Do the refugial areas of *B. reticulatus* correspond to the refugia of tree species typical of European broadleaf forest?
2. What is the role of the Caucasian region in the context of glacial survival and postglacial recolonization of the Western Palaearctic?
3. How did postglacial range expansion take place: pioneer- or phalanx-wise?
4. Does the population genetic structure of *B. reticulatus* relate to its ecology and behaviour?

MATERIAL AND METHODS

STUDY SPECIES

The genus *Bolitophagus* is represented in the Palaearctic by four species (*B. granulatus*, *B. interruptus*, *B. reticulatus* and *B. subinteger*; Iwan *et al.*, 2020). The most widespread species is *Bolitophagus reticulatus*, with a Palaearctic distribution but absent from central Mediterranean Europe. Its larvae and adults live in polypore fungi and are among the most frequent inhabitants of the tinder fungus *Fomes fomentarius* (Friess *et al.*, 2019). Adults of the beetle feed mainly on the spores of live basidiocarps, but are also commonly found in dead and deteriorated polypores, where its larvae develop (Midtgaard *et al.*, 1998). Experimental studies have shown that individuals can fly up to 125 km in a flight mill experiment (Jonsson, 2003). This high mobility is also supported by studies indicating gene-flow among populations at the local and regional scales (Jonsson *et al.*, 2003; Zytynska *et al.*, 2018). Although the beetle's main host is *Fomes fomentarius* (Nilsson, 1997), it has also been recorded from other polypores (e.g. *Phellinus nigricans*, *Fomitopsis pinicola*, *Piptoporus betulinus*, *Ganoderma applanatum*, *Laetiporus sulphureus* and *Daedaleopsis* spp.; Bouget *et al.*, 2019). *Fomes fomentarius* occurs on a range of broadleaf tree species, mainly beech (*Fagus* spp.), sometimes birch (*Betula* spp.), and rarely on others such as oak (*Quercus* spp.) and maple (*Acer* spp.).

SAMPLING

We collected 281 individuals of *B. reticulatus* from 57 beech forest sites across major parts of the beetle's western Palaearctic distribution range, including the Caucasus region. All specimens were morphologically determined to ensure conspecificity. We sampled five individuals at each site (wherever possible). Sampling was conducted during the years 2014, 2015 and 2017. We extracted individuals from sporocarps of *Fomes fomentarius* and subsequently stored them in 99% ethanol until further analyses. An overview of all

sampling sites including GPS coordinates is compiled in [Supporting Information Table S1](#). All individuals used in this study are stored at the Terrestrial Ecology Research Group, Technical University Munich (TUM), Freising, Germany.

MOLECULAR ANALYSES

DNA was extracted from head, thorax and fore legs applying the Qiagen DNeasy kit (Qiagen, Hilden, Germany) based on the standard protocol for tissue samples. Partial mitochondrial genes cytochrome oxidase subunit I (*cox1*), cytochrome *c* oxidase subunit II (*cox2*) and cytochrome *b* (*cob*) were amplified using the primer combinations and polymerase chain reaction (PCR) conditions described in Rangel López *et al.* (2018). Successfully amplified PCR products were purified with ExoSap (Thermo Fischer Scientific, Waltham, MA, USA) and subsequently sequenced in both directions by the Genomics Service Unit (GSU) of the Ludwig-Maximilians-Universität München (LMU), Germany. We successfully generated *cox1*, *cox2* and *cob* sequences for 208 individuals (out of the 281 individuals sampled). An overview of all sequences and GenBank accession numbers is given in [Supporting Information Table S2](#).

We successfully genotyped 17 polymorphic microsatellites for 255 individuals (out of the 281 individuals sampled) ([Supporting Information, Table S2](#)), with the same primers and conditions successfully applied in a previous study (Zytynska *et al.*, 2018). We used two multiplex combinations, each with eight or nine primer pairs, using three fluorescent dyes, 6-FAM, HEX and TAMRA, alongside the ROX size standard. PCR products were run on an ABI 3130xl Genetic Analyzer (Applied Biosystems – Life Technologies GmbH, Darmstadt, Germany) at the GSU of the LMU, Germany. Further details on protocols applied are given in Zytynska *et al.* (2018).

PHYLOGENETIC AND DEMOGRAPHIC ANALYSES

Forward and reverse reads of mtDNA sequences were assembled with GENEIOUS v.6.1.8 (<https://www.geneious.com>). After removing primer sequences and low-quality base calls from the sequence ends, multiple sequence alignment was performed per marker using the MUSCLE (Edgar, 2004a, b) algorithm as implemented in GENEIOUS.

Mitochondrial haplotypes were extracted from the aligned mitochondrial supermatrix in PEGAS v.0.13 (Paradis, 2010). Individuals with more than 100 missing sites were excluded and sites with missing or ambiguous data were disregarded. Haplotype

networks were inferred using an infinite sites model (i.e. uncorrected distance) with PEGAS and the spatial distribution of haplotypes was mapped with a combination of the R-packages MAPS v.3.3.0 (Becker *et al.*, 2018), RASTER v.3.1–5 (Hijmans, 2020) and GGLOT2 v.3.3.0 (Wickham, 2016). For the rare case that individual mitochondrial genes should have different evolutionary histories, haplotype networks per gene were also created using the same method.

A phylogenetic tree was inferred with IQ-TREE v.2.0-rc2 (Minh *et al.*, 2020). *Nalassus laevioctostriatus*, *Opatrum sabulosum* and *Eledonoprius armatus* were chosen as the outgroup based on a published phylogeny of tenebrionid beetles (Kergoat *et al.*, 2014). Respective sequences were obtained from NCBI GenBank (Supporting Information, Table S2). Data were partitioned into the three genes (*cox1*, *cox2*, *cob*) and their codon positions for a total of nine initial partitions were used as input for MODELFINDER (Kalyaanamoorthy *et al.*, 2017). This approach not only selects the best fitting substitution model for each partition, but also merges initial partitions according to their statistical properties to reduce parameter space. The top 10% of partition pairs were evaluated (option *-rcluster 10*). The heuristic tree search was repeated ten times. The best tree was chosen and rooted with *Opatrum sabulosum*. A total of 1×10^5 ultrafast bootstrap replicates were performed to provide branch support (Hoang *et al.*, 2018).

We performed Coalescent Bayesian Skyline analysis (Drummond *et al.*, 2005) with BEAST v.2.6.2 (Boukaert *et al.*, 2014). Outgroups were excluded for this analysis. An estimate of the *cox1* substitution rate in tenebrionid beetles ($3.54 \pm 0.38\%$ Myr⁻¹) (Papadopolou *et al.*, 2010) was used to calibrate the mitochondrial tree in time, using the mean estimate with a relaxed lognormal molecular clock model. Optimal models of nucleotide substitution and partition scheme were inferred with MODELFINDER (Kalyaanamoorthy *et al.*, 2017) in IQ-TREE; initial partitions were set to the three genes. The topology was linked across genes. Three independent Markov chain Monte Carlo (MCMC) chains were run for 8×10^7 generations, with sampling every 5×10^3 generations. Convergence of independent runs to similar values, stationarity and effective sample sizes were assessed in TRACER v.1.7.1 (Rambaut *et al.*, 2018) after removing a burn-in of 25% of samples. Based on the combined post-burn-in sample of all three runs, Bayesian Skyline plots were generated with TRACER and *ggplot2* v.3.3.0 (Wickham, 2016). The posterior sample of trees was summarized with TREEANNOTATOR from the BEAST software package, using maximum clade credibility and common ancestor heights.

ANALYSES OF POPULATION STRUCTURE

Analyses of population structure were done with microsatellite data using R v.4.0.2 (R Core Team, 2019) in R-STUDIO v.1.2.1335 (RStudio Team, 2018). Mean F_{ST} , G_{ST} , G'_{ST} and D_{Jost} were calculated globally and for refugia of beech (Table 1; Magri *et al.*, 2006; Schmitt & Varga, 2012) as basic descriptive molecular statistics of population differentiation per locus. Allelic richness and number of unique allele combinations, as well as mean observed and mean expected heterozygosity were calculated using the packages POPPR v.2.8.5 (Kamvar *et al.*, 2014, 2015), DIVERSITY v.1.9.90 (Keenan *et al.*, 2013) and ADEGENET v.2.1.2 (Jombart, 2008; Jombart & Ahmed, 2011). Pairwise F_{ST} -values were calculated for clusters inferred from total evidence (see below) using ADEGENET.

Populations of *B. reticulatus* were inferred with GENELAND v.4.9.2 (Guillot *et al.*, 2005b, 2012). GENELAND applies mixture models to infer clusters that are in Hardy–Weinberg equilibrium with linkage equilibrium between loci. We inferred genetic clusters using the uncorrelated frequency model based on three datasets: (1) microsatellites, (2) mitochondrial sequences and (3) the combination thereof (referred to as total evidence in the following). Single nucleotide polymorphisms (SNPs) were extracted from mitochondrial sequences using ADEGENET. The algorithm considers geographical coordinates of samples, assuming that populations are spatially separated and experience little gene flow (spatial model) (Guillot *et al.* 2005a). A spatial jitter of 0.00001 degrees was applied to avoid fixation of samples from one locality in the same cluster. MCMC chains were run for one million generations (five million for mtDNA), sampling every 1000th generation (5000th for mtDNA). Each analysis was repeated three times to ensure stability of the results. Log likelihood and log posterior density trace plots were inspected to ensure convergence and stationarity of runs and to identify potential outliers that were stuck in local optima using CODA v.0.19–3. The maximum number of populations was set to 50, which roughly corresponds to sampling localities. The maximum rate of the Poisson process was set to the number of individuals in the respective dataset. The maximum number of nuclei in the Poisson–Voronoi tessellation was set to twice the number of individuals, which is suggested for analyses under the spatial model. Null alleles were not filtered. Posterior samples of each repeat run were separately summarized using the *PostProcessChain*-function after removing a burn-in of 100 000 generations (400 000 for the total evidence dataset).

To test for isolation-by-distance, geographical distances were transformed from geographical coordinates to metres using the RASTER package (Hijmans 2020). Genetic distances were calculated using

ADEGENET (Jombart, 2008; Jombart & Ahmed, 2011). The distances were plotted against each other for all pairs of sampling locations and complemented by a two-dimensional density extrapolation to explore potential geographically and genetically isolated populations. Correlation of the distance matrices was statistically tested by a Mantel test as implemented in ADE4 (v.1.7–15; Chessel *et al.*, 2004). Significance was assessed by 10 000 randomizations.

RESULTS

The total concatenated alignment of the three mitochondrial genes consisted of 208 individuals and 1605 bp (*cox1*: 525 bp, *cox2*: 626 bp, *cob*: 454 bp). Missing data was 1.26, 2.98 and 1.19% for *cox1*, *cox2* and *cob*, respectively. Variation in the mitochondrial genes was generally low (Supporting Information, Fig. S1). The combined mitochondrial genes differed at 12 segregating sites (excluding sites with missing or ambiguous data), resulting in 12 mitochondrial haplotypes (haplotype diversity = 0.24, nucleotide diversity = 0.00024; 167 haplotypes were found using all sites with pairwise deletion of missing and ambiguous data). One haplotype was noticeably dominant in terms of individual number (in 87% of all individuals) and distribution range. This haplotype represented the centre of a star-shaped haplotype network (Fig. 1A, dark violet haplotype). The same haplotype networks were observed for single genes (not shown), except for two *cob*-haplotypes found in the Italian Abruzzi region that formed a common lineage. Other, less frequent haplotypes were regionally restricted with two exceptions that both occurred in the Carpathian Basin (Fig. 1A, yellow and red haplotypes). GENELAND identified four mitochondrial clusters which considerably overlapped geographically (Fig. 1B). The Crimean population represented a combination of haplotypes of the Caucasian and European haplotypes. This pattern was also discovered with Bayesian and maximum likelihood phylogenetic analyses.

The dated mitochondrial tree from Bayesian inference suggested four major and mostly well-supported clades (Fig. 2, clades A–D). An accumulation of recent diversification events was detected around 100 kya. Geographical turnover was high, so that specimens from the same region were rarely restricted to a single clade. The exception were the Caucasus specimens from Armenia, the easternmost sampling locality, which clustered in one clade together with one specimen from Crimea. Clades A and B largely included populations from more eastern locations and showed a connection to the most eastern records of *B. reticulatus* (Ukraine, Armenia). Those clades

also comprised specimens from eastern and northern Europe (Fig. 2). Clade C was largely restricted to the northern Carpathians, but likewise included specimens from Denmark and Sweden. Clade D comprised most specimens, originating from all over Europe except the far eastern localities on Crimea and Armenia. Nearly all populations sampled across France assembled into one lineage (part of clade D), only interspersed with three specimens from neighbouring German sites and one from Plitvice Lakes (Croatia). Posterior support values and crown diversification ages are given in Table 2. The mitochondrial tree from the maximum likelihood search largely confirmed the genetic clades obtained from Bayesian analysis, although some topological differences with little support were present (Supporting Information, Fig. S1, clades A–D). Bayesian Skyline analysis showed a marked increase in population size after 20 kya, with a recent tendency to reduced growth approximately 5 kya (Fig. 2).

Similar to our results obtained from mitochondrial data, global statistics of microsatellite data revealed generally low genetic diversity (Supporting Information, Table S3). Observed and expected heterozygosity were 0.46 and 0.78, respectively, on average across loci. Mean F_{ST} was 0.15, mean G_{ST} 0.28, mean G'_{ST} 0.64 and mean D_{Jost} 0.50. One nuclear cluster dominated the genetic structure based on polymorphic microsatellites (Fig. 1C, blue cluster). However, individual cluster composition differed substantially between mitochondrial and nuclear inferences. In contrast to results from mitochondrial sequences, nuclear clusters were spatially well separated. One exception was a disjunct Pyrenean–German cluster. This is in line with low population differentiation indices that were found between three clusters inferred from total evidence (mitochondrial, nuclear and geography): the F_{ST} value between a western and an eastern population was 0.14, while genetic exchange between them and a large central European cluster seemed to be substantial, resulting in F_{ST} values < 0.05 (Fig. S2). Furthermore, we found significant correlation of genetic and geographical distances among localities (Fig. 3) based on the Mantel test (expectation from simulation: -0.002 , variance: 0.039, observation: 0.738, $P < 0.001$).

DISCUSSION

The study of three mitochondrial genes and polymorphic microsatellites allowed us to reconstruct the postglacial dispersal pathways of *B. reticulatus*. Except for the European–Caucasian split, which may be due to the common isolation of beetle and broadleaf tree species, we found very little genetic differentiation. This is best

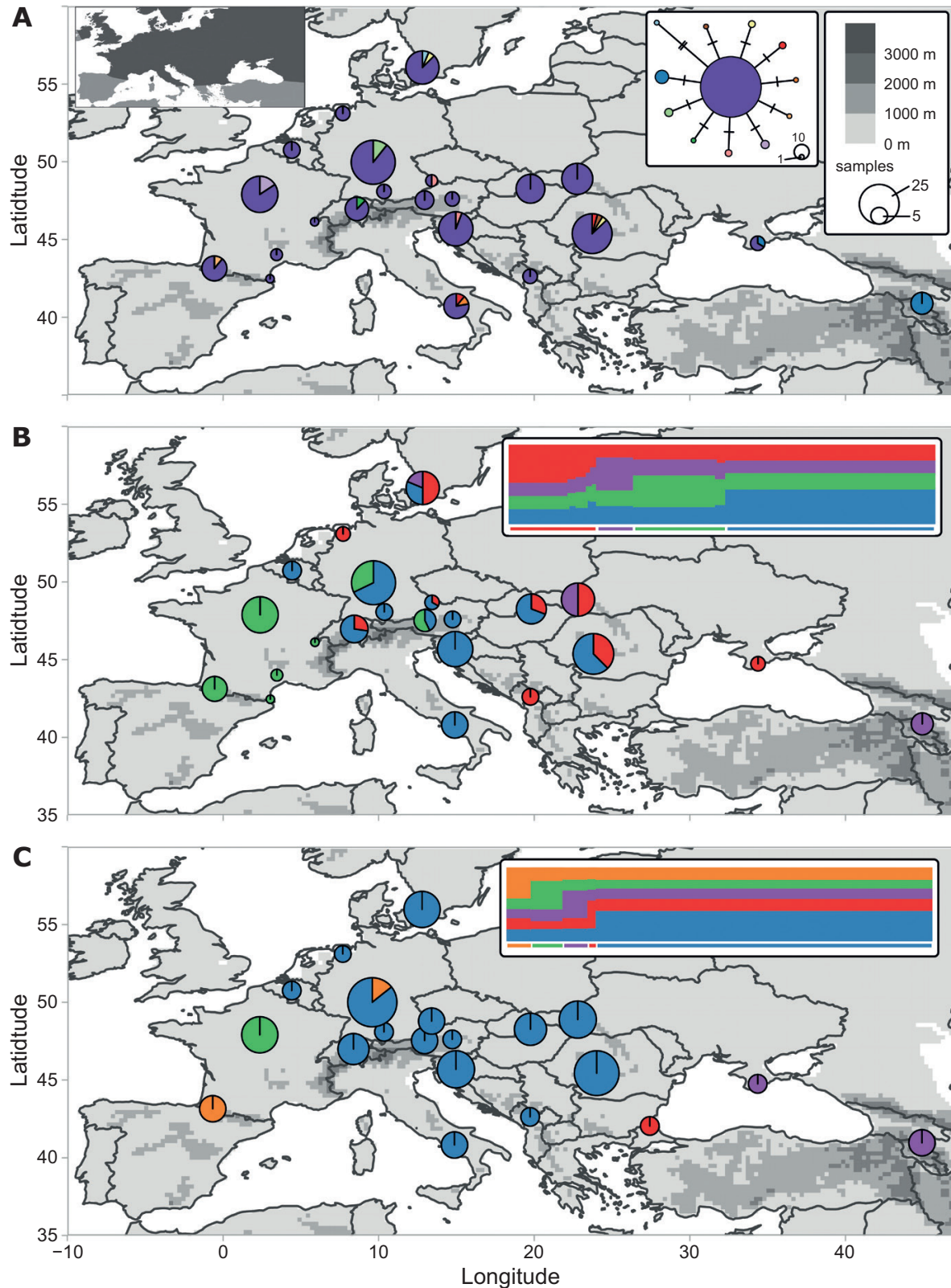


Figure 1. Spatial distribution of (A) 12 mitochondrial haplotypes and haplotype network (*cox1*, *cox2* and *cob*), (B) four mitochondrial genetic clusters from GENELAND analysis, and (C) five nuclear genetic clusters from GENELAND analyses

explained by genetic depletion in glacial refugia and rapid postglacial dispersal out of these refugia.

THE EUROPEAN–CAUCASIAN SPLIT

mtDNA and microsatellite analysis showed that the clade restricted to the Caucasus region was clearly distinguishable from the European clade. These genetic signatures and the early divergence of the Caucasus lineage (~500 kya) suggest the existence of a refuge area south of the Great Caucasus. This finding is in line with previous molecular biogeographical studies on other species in which European and Caucasian populations were included (see, e.g., Filipova-Marinkova, 1995; Pavlova et al., 2005; Hansson et al., 2008). Molecular analysis has identified a sister species relationship between European beech (*Fagus sylvatica*) and Oriental beech (*Fagus orientalis*) (Renner et al., 2016), which are distributed in Europe and the Caucasus, respectively (www.euforgen.org; accessed December 2020). The same isolating forces that caused speciation in the two beech species are likely to be responsible for the intraspecific differentiation in *B. reticulatus*. Furthermore, our data indicated the Crimean region as being the contact zone between European populations and the populations of the Great Caucasus, as also identified in previous studies, for example for land snails (Neiber & Hausdorf, 2017).

REFUGIA ACROSS CENTRAL EUROPE

Infrequent mitochondrial haplotypes were regionally restricted, with two exceptions, both for the Carpathian Basin. This suggests a glacial refugium of *B. reticulatus* on the Balkan Peninsula, and postglacial range expansions across the south-eastern European region, with major areas on the Balkan Peninsula, including the foothills of the Carpathians and areas of central Europe. This scenario was also supported by phylogenetic inference, and is in line with a range of previous studies (reviewed by Schmitt, 2007). The postglacial range expansions from the Balkan Peninsula across major parts of eastern central Europe coincide with the phylogeography of the European meadow grasshopper *Chorthippus parallelus* (Lunt et al., 1998), which gives its name to one of the three paradigms stated by Hewitt (1996, 1999, 2000). Very similar patterns of postglacial expansion are known for several other species, including crested newts

(*Triturus cristatus*) (Wallis & Arntzen, 1989; Wielstra et al., 2013) and European beech (*F. sylvatica*) (Magri et al., 2006; Magri, 2008).

Given the generally high spatial admixture revealed from mtDNA in *B. reticulatus*, it is noteworthy that phylogenetic analyses assigned all but two specimens from France to one clade, although this is not well supported (Fig. 2). Likewise, GENELAND clustered all individuals from France into one cluster when used with mtDNA data and suggested a connection to central Europe (Fig. 1B). Potential scenarios shaping such a pattern are extra-Mediterranean glacial refugia located within the Massif Central or the foothills of the Pyrenees with subsequent postglacial range expansion. This is a frequently observed pattern in biogeographical studies of organisms of temperate Europe. However, the low genetic diversity in France suggests a bottleneck effect during the last glacial maximum and thus, probably, a small refugium. The multiple extra-Mediterranean glacial refugia found for *B. reticulatus* (e.g. the Carpathian Basin, Massif Central/Pyrenees) match findings for the various European broadleaf tree species which are exploited by *Fomes fomentarius*. For example, molecular data for European beech also indicate past refugia in the foothills of the Pyrenees (Magri 2008). Other studies suggest that various tree species of the European broadleaf forest expanded early after the last glacial maximum northwards, or even survived in more northern extra-Mediterranean refugia (Chlebicki & Lorenc, 1997; Svenning et al., 2008; Schmitt & Varga, 2012).

RANGE EXPANSIONS

The observed genetic patterns show that *B. reticulatus* has been restricted to areas with beech-dominated broadleaf forest that provided good conditions for the tinder fungus (Schwarze, 1994). The tinder fungus and *B. reticulatus* are capable dispersers and probably exhibit similar postglacial population expansion. The chronogram in our study indicated an accumulation of diversification events in *B. reticulatus* associated with the beginning of the last ice-age around 100 kya; the median estimate of the onset of population growth was about 20 kya, which coincides with the end of the last glacial maximum. This population growth pattern inferred from mtDNA suggests range expansions and population increase significantly before the period of colonization by beech trees, as

of polymorphic microsatellites. The size of the pie charts represents the number of samples; the size of the circles in the haplotype network represents the number of respective haplotypes. Pie charts may summarize several close by localities. The inset in A shows the approximate distribution of *Bolitophagus reticulatus* in the study area (own data and www.gbif.org). Insets in B and C show membership probabilities (y-axis) of individuals (x-axis) to inferred clusters, which are colour coded for the respective maps. Coloured bars below the plot indicate assigned group membership.

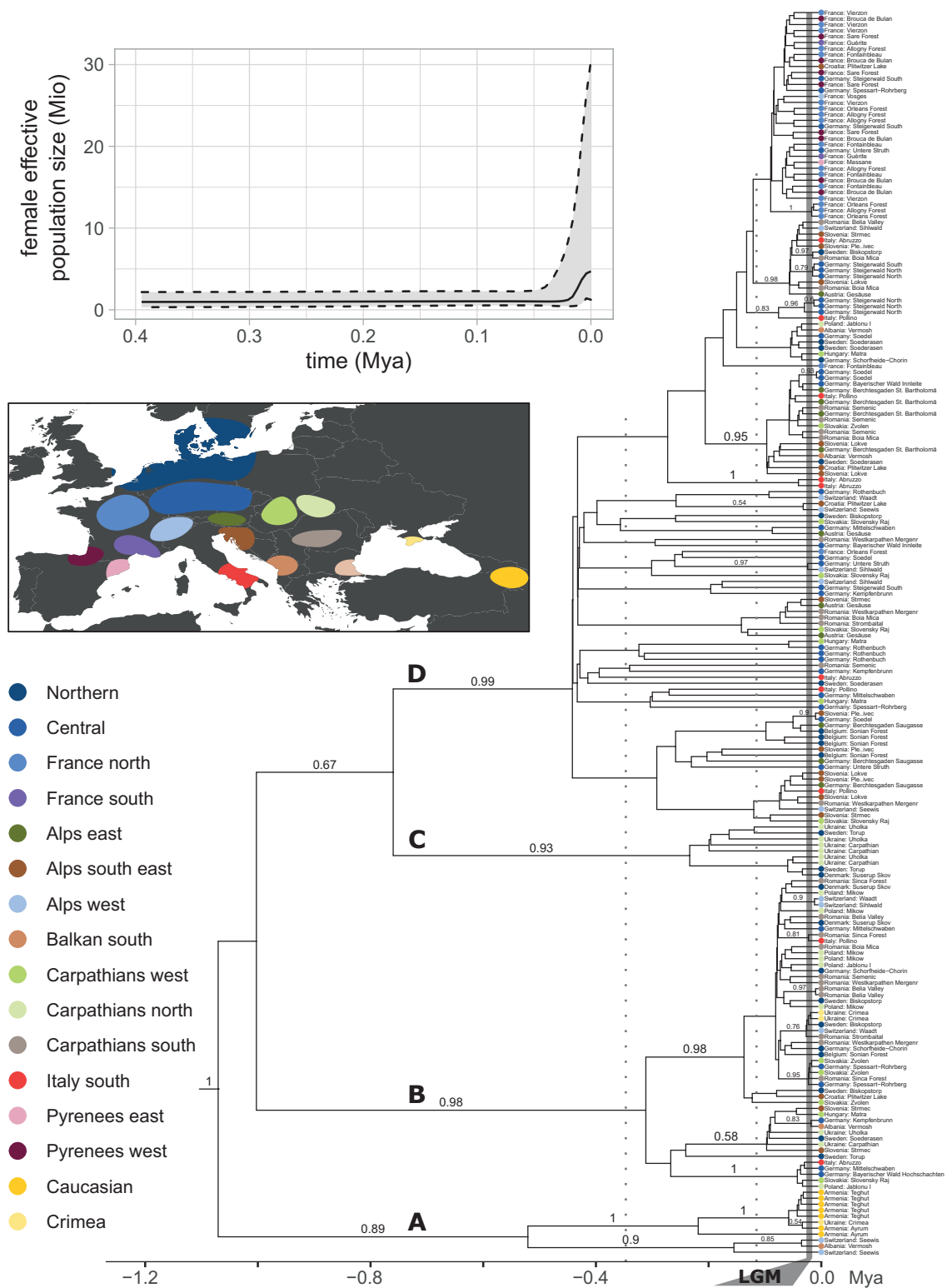


Figure 2. Time-calibrated phylogenetic tree from Bayesian analysis of mitochondrial DNA sequences (*cox1*, *cox2* and *cob*). Vertical dotted lines indicate the onset of the last glacial periods. The vertical grey line marks the last glacial maximum. Colour dots at the trees' tips illustrate geographical origins of the sample. Coloured areas on the map roughly encircle sampling points of the present study and include refugia of European and Oriental beech. Upper inset: Bayesian Skyline plot showing demographic change in female effective population size over time, assuming a generation time of 1 year.

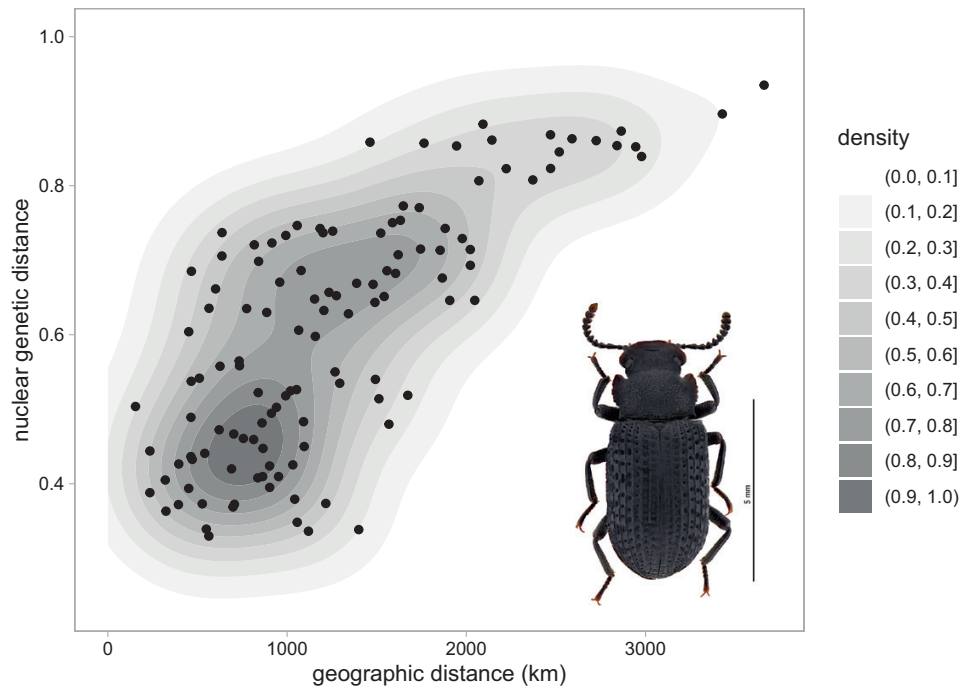


Figure 3. Pairwise geographical and genetic distance between localities illustrate isolation by distance. Nuclear genetic distance was inferred from microsatellite data. Shades of grey indicate data point density.

Table 1. Investigated regions and genetic diversities obtained for all populations analysed. Given are the coordinates in decimal format (WGS84), the number of mitochondrial DNA samples n_{mt} , haplotypes HT , nuclear DNA samples n_n , alleles A and allele combinations, as well as observed and expected heterozygosity, H_o , and H_e respectively

Region	n_{mt}	HT	n_n	A	Comb.	H_o	H_e
Alps east	8	1	15	95	106	0.35	0.61
Alps south-east	17	2	20	146	195	0.50	0.77
Alps west	9	2	14	138	150	0.48	0.75
Balkan east	na	na	5	47	50	0.48	0.48
Balkan south	3	1	5	86	76	0.63	0.70
Carpathians north	14	1	20	129	175	0.48	0.70
Carpathians south	23	4	29	156	223	0.46	0.72
Carpathians west	12	1	15	97	122	0.44	0.65
Caucasian	7	1	10	38	43	0.16	0.24
Central	33	3	50	177	299	0.51	0.74
Crimea	3	2	5	49	51	0.39	0.48
France north	19	2	19	93	142	0.50	0.62
France south	2	1	na	na	na	na	na
Italy south	9	3	10	102	117	0.51	0.72
Northern	23	3	28	149	228	0.45	0.75
Pyrenees east	1	1	na	na	na	na	na
Pyrenees west	9	2	10	71	82	0.42	0.53

na, not applicable.

derived from palaeontological evidence (Magri *et al.*, 2008). Thus, the association between *B. reticulatus* and the tinder fungus might have occurred much

earlier, and independently of beech. A plausible scenario is that expansion depended on pioneer tree species such as birch, although in temperate

Table 2. Crown ages of major lineages from Bayesian divergence dating (compare with Fig. 2)

Node	Posterior clade support	Median age (kya)	Mean age (kya)	95% HPD interval (kya)
Root	1.00	971.8	1070.5	398.8–1960.6
A	0.89	400.3	456.3	107.1–928.7
B	0.98	279.2	308.2	102.3–582.2
C + D	0.67	585.7	644.8	234.5–1181.8
C	0.93	174.5	216.1	24.2–515.5
D	0.99	389.2	434.0	153.8–818.5

HPD, highest posterior density.

European forests beech is now the main host for the tinder fungus.

The weak genetic differentiation, alongside high geographical turnover of mtDNA and low F_{ST} values among regional clusters, as well as the lack of gradual loss of genetic diversity along potential colonization pathways, allows us to infer the expansion pattern of *B. reticulatus*. While pioneer processes lead to signatures of gradual loss of genetic diversity in the course of colonization (Ibrahim *et al.*, 1996), phalanx-wise colonization results in a lack of genetic signatures along colonization routes (Hewitt, 2000). The observed lack of genetic differentiation, in combination with the isolation by distance pattern, supports a phalanx-wise colonization of Europe and reflects the strong mobility of *B. reticulatus* (Jonsson, 2003). Similar genetic signatures have also been found for the longhorn beetle *Rosalia alpina* (Drag *et al.*, 2018), which inhabits similar beech-dominated forests. Our data underline the ability of *B. reticulatus* to rapidly colonize new habitats and the frequent individual exchanges among local populations, both of which counteract potential genetic differentiation.

ACKNOWLEDGEMENTS

We greatly appreciate the valuable comments by Thomas Schmitt on an earlier version of the manuscript. We thank Sarah Sturm, Jose Angel Rangel Lopez and Yasemin Guenay for laboratory work. Mathis Bortfeld, Radosław Gil, Simon Thorn and Barbara Winter kindly contributed further samples. This project was financed by the Bayerisches Staatsministerium für Ernährung, Landwirtschaft und Forst, Munich, Germany (Grant L55) and the Technical University Munich, Germany. W.U. was supported by an internal Excellence Initiative - Research University (IDUB) grant of the Nicolaus Copernicus University, Toruń, Poland. We thank the LWF and the Bavarian State Forestry BaySF for fruitful collaboration. In particular, we want to thank Ulrich Mergner and Nadja Simons for their help in the field. We are grateful to three reviewers for valuable

comments on the manuscript. The authors declare they have no conflicts of interest.

REFERENCES

- Becker RA, Wilks AR (Original S code), Brownrigg R, Minka TP, Deckmyn A (R version). 2018. *maps: Draw Geographical Maps. R package version 3.3.0*. Available at: <https://CRAN.R-project.org/package=maps>
- Bouget C, Brustel H, Noblecourt T, Zagatti P. 2019. *Les Coléoptères saproxyliques de France – Catalogue écologique illustré*. Paris: Muséum national d'Histoire naturelle (Patrimoines naturels; 79).
- Boukaert R, Heled J, Kühnert D, Vaughan T, Wu CH, Xie D, Suchard MA, Rambaut A, Drummond AJ. 2014. BEAST 2: a software platform for Bayesian evolutionary analysis. *PLoS Computational Biology* **10**: 1–6.
- Brunet J, Fritz Ö, Richnau G. 2010. Biodiversity in European beech forests – a review with recommendations for sustainable forest management. *Ecological Bulletin* **55**: 77–94.
- Chessel D, Dufour A, Thioulouse J. 2004. The ade4 Package – I: One-table methods. *R News* **4**: 5–10.
- Chlebicki A, Lorenc MW. 1997. Subfossil *Fomes fomentarius* from a Holocene fluvial deposit in Poland. *The Holocene* **7**: 101–103.
- Drag L, Hauck D, Bérces S, Michalciewicz J, Jelaska LS, Aurenhammer S, Cizek L. 2015. Genetic differentiation of populations of the threatened saproxylic beetle *Rosalia longicorn*, *Rosalia alpina* (Coleoptera: Cerambycidae) in Central and South-east Europe. *Biological Journal of the Linnean Society* **116**: 911–925.
- Drag L, Hauck D, Pokluda P, Zimmermann K, Cizek L. 2011. Demography and dispersal ability of a threatened saproxylic beetle: a mark-recapture study of the *Rosalia longicorn* (*Rosalia alpina*). *PLoS One* **6**: e21345.
- Drag L, Hauck D, Rican O, Schmitt T, Shovkoon DF, Godunko RJ, Curletti G, Cizek L. 2018. Phylogeography of the endangered saproxylic beetle *Rosalia longicorn* *Rosalia alpina* (Coleoptera, Cerambycidae), corresponds with its main host, the European beech (*Fagus sylvatica*, Fagaceae). *Journal of Biogeography* **45**: 2631–2644.

- Drummond AJ, Rambaut A, Shapiro B, Pybus OG. 2005. Bayesian coalescent inference of past population dynamics from molecular sequences. *Molecular Biology and Evolution* **22**: 1185–1192.
- Edgar RC. 2004a. MUSCLE: multiple sequence alignment with high accuracy and high throughput. *Nucleic Acids Research* **32**: 1792–1797.
- Edgar RC. 2004b. MUSCLE: a multiple sequence alignment method with reduced time and space complexity. *BMC Bioinformatics* **5**: 113.
- Filipova-Marinova M. 1995. Late Quaternary history of the genus *Fagus* in Bulgaria. In: Bozilova E, Tonkov S, eds. *Advances in Holocene palaeoecology in Bulgaria*. Sofia: Pensoft Publishers, 84–95.
- Friess N, Müller JC, Abrego N, Aramendi P, Bässler C, Bouget C, Brin A, Bussler H, Georgiev K, Gil R, Gossner MM, Heilmann-Clausen J, Isaacson G, Krištín A, Lachat T, Larrieu L, Los S, Magnanou E, Maringer A, Mergner U, Mikolas M, Opgenoorth L, Schmidl J, Svoboda M, Thorn S, Vrezec A, Vanderkhoven K, Winter B, Wagner T, Zapponi L, Brandl R, Seibold S. 2019. The species-rich arthropod communities in fungal fruitbodies are weakly structured by climate and biogeography across European beech forests. *Diversity and Distributions* **25**: 783–796.
- Giesecke T, Brewer S, Finsinger W, Leydet M, Bradshaw RHW. 2017. Patterns and dynamics of European vegetation change over the last 15 000 years. *Journal of Biogeography* **44**: 1441–1456.
- Guillot G, Estoup A, Mortier F, Cosson JF. 2005a. A spatial statistical model for landscape genetics. *Genetics* **170**: 1261–1280.
- Guillot G, Mortier F, Estoup A. 2005b. Geneland: a program for landscape genetics. *Molecular Ecology Notes* **5**: 712–715.
- Guillot G, Renaud S, Ledevin R, Michaux J, Claude J. 2012. A unifying model for the analysis of phenotypic, genetic and geographic data. *Systematic Biology*, **61**: 897–911.
- Hansson B, Hasselquist D, Tarka M, Zehndtjev P, Bensch S. 2008. Postglacial colonisation patterns and the role of isolation and expansion in driving diversification in a passerine bird. *PLoS ONE* **3**: e2794.
- Hewitt GM. 1996. Some genetic consequences of ice ages, and their role in divergence and speciation. *Biological Journal of the Linnean Society* **58**: 247–276.
- Hewitt GM. 1999. Post-glacial recolonization of European biota. *Biological Journal of the Linnean Society* **68**: 87–112.
- Hewitt GM. 2000. The genetic legacy of the Quaternary ice ages. *Nature* **405**: 907–913.
- Hijmans RJ. 2020. raster: Geographic Data Analysis and Modelling. R package version 3.1–5. Available at: <https://CRAN.R-project.org/package=raster>
- Hoang DT, Chernomor O, von Haeseler A, Minh BQ, Vinh LS. 2018. UFBoot2: improving the ultrafast bootstrap approximation. *Molecular Biology and Evolution* **35**: 518–522.
- Ibrahim KM, Nichols RA, Hewitt GM. 1996. Spatial patterns of genetic variation generated by different forms of dispersal during range expansion. *Heredity* **77**: 282–291.
- Iwan D, Löbl I, Bouchard P, Bousquet Y, Kamiński M, Merkl O, Ando K, Schawaller W. 2020. Family Tenebrionidae Latreille, 1802. In: Iwan D, Löbl I, eds. *Catalogue of Palaearctic Coleoptera, Volume 5, Tenebrionoidea. Revised and updated second edition*. Leiden: Brill NV, 27–641.
- Jiménez-Alfaro B, Girardello M, Chytrý M, Svenning JC, Willner W, Gégout JC, Agrillo E, Campos JA, Jandt U, Kącki Z, Šilc U, Slezák M, Tichý L, Tsiripidis I, Turtureanu PD, Ujházyová M, Wohlgemuth T. 2018. History and environment shape species pools and community diversity in European beech forests. *Nature Ecology & Evolution* **2**: 483–490.
- Jombart T. 2008. adegenet: a R package for the multivariate analysis of genetic markers. *Bioinformatics* **24**: 1403–1405.
- Jombart T, Ahmed I. 2011. adegenet 1.3-1: new tools for the analysis of genome-wide SNP data. *Bioinformatics* **27**: 3070–3071.
- Jonsson M. 2003. Colonisation ability of the threatened tenebrionid beetle *Oplocephala haemorrhoidalis* and its common relative *Bolitophagus reticulatus*. *Ecological Entomology* **28**: 159–167.
- Jonsson M, Johannesen J, Seitz A. 2003. Comparative genetic structure of the threatened tenebrionid beetle *Oplocephala haemorrhoidalis* and its common relative *Bolitophagus reticulatus*. *Journal of Insect Conservation* **7**: 111–124.
- Kalyanamoorthy S, Minh BQ, Wong TKF, von Haeseler A, Jermin LS. 2017. ModelFinder: fast model selection for accurate phylogenetic estimates. *Nature Methods* **14**: 587–589.
- Kamvar ZN, Brooks JC, Grünwald NJ. 2015. Novel R tools for analysis of genome-wide population genetic data with emphasis on clonality. *Frontiers in Genetics* **6**: 208.
- Kamvar ZN, Tabima JF, Grünwald NJ. 2014. Poppr: an R package for genetic analysis of populations with clonal, partially clonal, and/or sexual reproduction. *PeerJ* **2**: e281.
- Keenan K, McGinnity P, Cross TF, Crozier WW, Prodöhl PA. 2013. diveRsity: An R package for the estimation of population genetics parameters and their associated errors. *Methods in Ecology and Evolution* **4**: 782–788.
- Kergoat GJ, Soldati L, Clamens AL, Jourdan H, Jabbour-Zahab R, Genson G, Bouchard P, Condamine FL. 2014. Higher level molecular phylogeny of darkling beetles (Coleoptera: Tenebrionidae). *Systematic Entomology* **39**: 486–499.
- Lunt DH, Ibrahim KM, Hewitt GM. 1998. mtDNA phylogeography and postglacial patterns of subdivision in the meadow grasshopper *Chorthippus parallelus*. *Heredity* **80**: 633–641.
- Magri D. 2008. Patterns of post-glacial spread and the extent of glacial refugia of European beech (*Fagus sylvatica*). *Journal of Biogeography* **35**: 450–463.
- Magri D, Vendramin GG, Comps B, Dupanloup I, Geburek T, Gomory D, Latalowa M, Litt T, Paule L, Roure JM, Tantau I, van der Knaap WO, Petit RJ, de Beaulieu JL.

2006. A new scenario for the Quaternary history of European beech populations: palaeobotanical evidence and genetic consequences. *New Phytologist* **171**: 199–221.
- Midtgaard F, Rukke BA, Sverdrup-Thygesen A. 1998. Habitat use of the fungivorous beetle *Bolitophagus reticulatus* (Coleoptera: Tenebrionidae): effects of basidiocarp size, humidity and competitors. *European Journal of Entomology* **95**: 559–570.
- Minh BQ, Schmidt HA, Chernomor O, Schrempf D, Woodhams MD, von Haeseler A, Lanfear R. 2020. IQ-TREE 2: new models and efficient methods for phylogenetic inference in the genomic era. *Molecular Biology and Evolution* **37**: 1530–1534.
- Müller J, Brunet J, Brin A, Bouget C, Brustel H, Bussler H, Förster B, Isacson G, Köhler F, Lachat T, Gossner MM. 2013. Implications from large-scale spatial diversity patterns of saproxylic beetles for the conservation of European Beech forests. *Insect Conservation and Diversity* **6**: 162–169.
- Neiber MT, Hausdorf B. 2015. Phylogeography of the land snail genus *Circassina* (Gastropoda: Hygromiidae) implies multiple Pleistocene refugia in the western Caucasus region. *Molecular Phylogenetics and Evolution* **93**: 129–142.
- Neiber MT, Hausdorf B. 2017. Molecular phylogeny and biogeography of the land snail genus *Monacha* (Gastropoda, Hygromiidae). *Zoologica Scripta* **46**: 308–321.
- Nilsson T. 1997. Survival and habitat preferences of adult *Bolitophagus reticulatus*. *Ecological Entomology* **22**: 82–89.
- Papadopoulou A, Anastasiou I, Vogler AP. 2010. Revisiting the insect mitochondrial molecular clock: the mid-Aegean trench calibration. *Molecular Biology and Evolution* **27**: 1659–1672.
- Paradis E. 2010. pegas: an R package for population genetics with an integrated-modular approach. *Bioinformatics* **26**: 419–420.
- Pavlova A, Zink RM, Rohwer S, Koblik EA, Red'kin YA, Fadeev IV, Nesterov EV. 2005. Mitochondrial DNA and plumage evolution in the white wagtail *Motacilla alba*. *Journal of Avian Biology* **36**: 322–336.
- Pons JM, Oliso G, Cruaud C, Fuchs J. 2011. Phylogeography of the Eurasian green woodpecker (*Picus viridis*). *Journal of Biogeography* **38**: 311–325.
- Pott R. 2000. Die Entwicklung der europäischen Buchenwälder in der Nacheiszeit. *Rundgespräche der Kommission für Ökologie* **18**: 49–75.
- R Core Team. 2019. *R: A language and environment for statistical computing*. Vienna: R Foundation for Statistical Computing. Available at: <https://www.R-project.org/>.
- Rambaut A, Drummond AJ, Xie D, Baele G, Suchard MA. 2018. Posterior summarization in Bayesian phylogenetics using Tracer 1.7. *Systematic Biology* **67**: 901–904.
- Rangel López JÁ, Husemann M, Schmitt T, Kramp K, Habel JC. 2018. Mountain barriers and trans-Saharan connections shape the genetic structure of *Pimelia* darkling beetles (Coleoptera: Tenebrionidae). *Biological Journal of the Linnean Society* **124**: 547–556.
- Renner SS, Grimm GW, Kapli P, Denk T. 2016. Species relationships and divergence times in beeches: new insights from the inclusion of 53 young and old fossils in a birth–death clock model. *Philosophical Transactions of the Royal Society B* **371**: 20150135.
- RStudio Team. 2018. *RStudio: Integrated Development for R*. Boston: RStudio, Inc. Available at: <http://www.rstudio.com/>.
- Rukke BA. 2000. Effects of habitat fragmentation: increased isolation and reduced habitat size reduces the incidence of dead wood fungi beetles in a fragmented forest landscape. *Ecography* **23**: 492–502.
- Saltré F, Saint-Amant R, Gritti ES, Brewer S, Gaucherel C, Davis BAS, Chuine I. 2013. Climate or migration: what limited European beech post-glacial colonization? *Global Ecology and Biogeography* **22**: 1217–1227.
- Schmitt T. 2007. Molecular biogeography of Europe: Pleistocene cycles and postglacial trends. *Frontiers in Zoology* **4**: 11.
- Schmitt T, Seitz A. 2001. Allozyme variation in *Polyommatus coridon* (Lepidoptera: Lycaenidae): identification of ice-age refugia and reconstruction of post-glacial expansion. *Journal of Biogeography* **28**: 1129–1136.
- Schmitt T, Varga Z. 2012. Extra-Mediterranean refugia: the rule and not the exception? *Frontiers in Zoology* **9**: 22.
- Schwarze F. 1994. Wood rotting fungi: *Fomes fomentarius* (L.: Fr.) Fr.: Hoof or tinder fungus. *Mycologist* **8**: 32–34.
- Stauffer C, Lakatos F, Hewitt GM. 1999. Phylogeography and postglacial colonization routes of *Ips typographus* L. (Coleoptera, Scolytidae). *Molecular Ecology* **8**: 763–773.
- Svenning JC, Normand S, Kageyama M. 2008. Glacial refugia of temperate trees in Europe: insights from species distribution modelling. *Journal of Ecology* **96**: 1117–1127.
- Tarkhnishvili D, Gavashelishvili A, Mumladze L. 2012. Palaeoclimatic models help to understand current distribution of Caucasian forest species. *Biological Journal of the Linnean Society* **105**: 231–248.
- Wallis GP, Arntzen JW. 1989. Mitochondrial-DNA variation in the crested newt superspecies: limited cytoplasmic gene flow among species. *Evolution* **43**: 88–104.
- Wickham H. 2016. *ggplot2: elegant graphics for data analysis*. New York: Springer.
- Wielstra B, Baird AB, Arntzen JW. 2013. A multimarker phylogeography of crested newts (*Triturus cristatus* superspecies) reveals cryptic species. *Molecular Phylogenetics and Evolution* **67**: 167–175.
- Zytyńska SE, Doerfler I, Gossner MM, Sturm S, Weisser WW, Müller J. 2018. Minimal effects on genetic structuring of a fungus-dwelling saproxylic beetle after recolonisation of a restored forest. *Journal of Applied Ecology* **55**: 2933–2943.

SUPPORTING INFORMATION

Additional Supporting Information may be found in the online version of this article at the publisher's web-site:

Table S1. Sampling sites and genetic diversity measures.

Table S2. GenBank accession numbers for mtDNA sequences and microsatellite data.

Table S3. Global statistics of microsatellite data.

Figure S1. Mitochondrial tree from maximum likelihood analysis.

Figure S2. Spatial distribution of three clusters inferred by GENELAND based on total evidence.

SHARED DATA

The mtDNA sequences underlying this article are available in the GenBank Nucleotide Database at www.ncbi.nlm.nih.gov/genbank/, and can be accessed with the accession numbers MH383529–MH383770 for *cob*, MH383771–MH384020 for *cox1* and MH384021–MH384258 for *cox2*. Sequence alignments and phylogenetic trees are available in TreeBase at <http://purl.org/phylo/treebase/phylows/study/TB2:S27736>. Microsatellite data are available in the online supplementary material (Table S2).